成蹊大学理工学研究報告
J. Fac. Sci.Tech., Seikei Univ.
Vol.55 No.1 (2018)pp.1-10

ウェブスターのホーン方程式における摂動論による高精度計算手法

濱野 慶太*1, 坂本 昇一*2, 富谷 光良*3

Highly Accurate Perturbative Method for Webster's Horn Equation

Keita HAMANO*1, Shoichi SAKAMOTO*2, Mitsuyoshi TOMIYA*3

ABSTRACT：Applying mathematical and quantum mechanical techniques, this study develops numerical solutions to Webster's horn equation, which describes the sound inside brass instruments in acoustics. The wavenumbers and wave functions of the modes in the system are evaluated by perturbation theory, assuming a solvable system with relatively small perturbations. An obvious solvable example is a straight pipe, whose wavenumbers can be perturbed by varying the radius of the horn. Maintaining the second-order corrections, the method generated astonishingly accurate results for varying horn shapes. Moreover, in tests of various pipe shapes, the perturbation method required far fewer computational resources than the finite element method. Two analytically solvable shapes and two non-solvable models (one of them is a periodic shape described by a trigonometric function) are analyzed. The results imply the applicability of the method to highly non-solvable systems.

Keywords：Webster's Horn Equation, Perturbation Theory, Brass Instruments, High Accuracy Solutions

(Received June 8, 2018)

1 INTRODUCTION

Lately, sophisticated tools designed for solving nonlinear problems have been successfully applied to studies of wind instruments. In particular, these tools can analyze the resonance phenomena and predict the sound propagation and reflection inside finite spaces such as pipes.[1] A typical application reveals the dynamic function of the register hole on the clarinet, which comprises a two-delay system.[2]

However, the sound making methods and resonance mechanisms of musical instruments have not been sufficiently unravelled.[1),3)] Even simply structured instruments such as recorders remain incompletely understood. Therefore, investigating these mechanisms is essential for the research and development of wind instruments. One promising approach toward a precise and manageable design method for specific instruments is the technique in quantum mechanics, which naturally describes wave dynamics. The expected close relationship between acoustics and quantum mechanics should exactly fulfil our intention.[4)]

As a representative brass instrument, a trumpet can be divided into three parts: a lead pipe, a piston unit and a horn (also called a bell).[1),3)] The lead pipe amplifies the sound, the pistons control the pitch and the horn acts as a speaker. Additionally, the horn is easily manufactured in various sizes and shapes, and from a variety of materials. Indeed, the horn is merely the aperture of the instrument, and its tone is easily supplemented by distinguishing characteristics.

The normal modes and frequencies of the horn can be altered by adjusting the horn structure. Understanding the relationship between the modes and structure of a horn is crucial in instrument manufacture. The pressure changes inside the horn are well approximated by Webster's horn equation,[5),6)] which is generally solved by numerical methods; analytical solutions can be obtained only in some special cases. However, the balance of the musical instrument can be disrupted by

*1：理工学研究科物質生命理工学専攻修士学生
*2：物質生命理工学専攻助教
*3：物質生命理工学専攻教授(tomiya@st.seikei.ac.jp)

numerical errors, which are unavoidable in numerical analyses.

In this work, we approach the acoustics in a horn from a quantum mechanics perspective. The perturbation method, which derives the solutions of Schrödinger equation with small perturbations,[7] can evaluate the modes of brass instruments.[8),9)] For various horn shapes, the approximate solutions computed by perturbation theory are far more accurate than those of ordinary numerical methods such as the finite element method (FEM)[10),11)] and the eigenfunction expansion method.[6),12),13)]

Although quantum physics underlies the modern science of the twentieth century, the perturbation method was originally developed to explain the motions of planets in the solar system, and stars in galaxies, and similar problems in classical astrophysics.[14)]

The Webster's equation, which describes the sound in a pipe with varying radius,[10)] can be mathematically likened to a perturbed Schrödinger equation.[8),9)] Thus, perturbation theory can be applied to the acoustics of brass instruments. Perturbation theory divides the system into a non-perturbative and a perturbative part. The former part usually admits an exact solution, whereas the latter is expressed as an asymptotic series expansion with respect to the perturbation term, assuming a sufficiently small perturbation strength. This formulation gives an approximate solution to systems with no exact analytical solutions.

Our system treats the horn structure as a straight pipe (exactly solvable) with some deformations (perturbations), which model the deformation of the stationary states. The method returns precise results for the rotation volumes (one revolution around the x-axis) of four horn structures, proportional to e^{-x}, $1/x$, $3+\cos x$, and $\ln(x)$ (x>0). Ordinary numerical methods such as FEM usually perform best in the lower frequency region, because the lattice constant must be smaller than the wavelength. In contrast, the perturbative method usually achieves better results in the higher frequency region than FEM.

2 WEBSTER'S EQUATION AND SCHRÖDINGER EQUATION

Sound is the physical phenomenon manifesting from the propagation of pressure changes through a medium such as air. If the wavelength is sufficiently larger than the horn diameter, the propagation becomes essentially one-dimensional and is regarded as a plane wave. Taking the x-coordinates along the center axis of the horn, and the two apertures (bottoms) at $x = a, b$, Webster's equation of the sound pressure is given by [15]:

$$\frac{\partial}{\partial x}\left(S(x)\frac{\partial P(x,t)}{\partial x}\right)=\frac{S(x)}{c^2}\frac{\partial^2 P(x,t)}{\partial t^2} \quad , \tag{1}$$

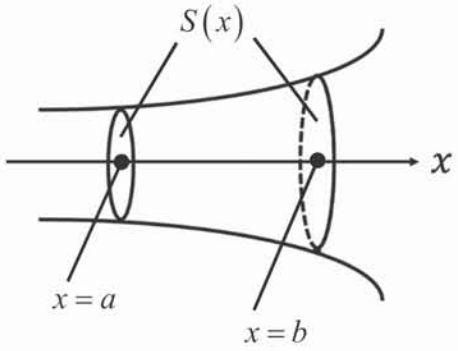

FIG. 1. Outline of the pipe to be used in Webster's equation

where $P(x,t)$ is taken here as the acoustic or excess pressure, which is the pressure difference from the static one, $S(x)$ represents the varying cross-sectional area of the horn part (FIG.1), c is the speed of sound, and t is time.

The Schrödinger equation for an exactly solvable system with Hamiltonian H_0 is given by

$$H_0\psi_{0,n} = E_{0,n}\psi_{0,n} \, , \tag{2}$$

where $\psi_{0,n}$ is an eigenstate of the solvable system with eigen-energy $E_{0,n}$. The Schrödinger equation with a small perturbation H_1 then becomes

$$H\psi_n = (H_0 + H_1)\psi_n = E\psi_n \quad . \tag{3}$$

The term H_1 can be any suitable term, such as a potential energy, an interaction term or a perturbative part.

Quantum mechanics is a powerful tool for handling systems that satisfy the perturbation equation (3). Perturbation theory derives the energy spectra and wavefunctions of perturbative systems from those of the solvable system, adding correction terms generated by expanding the perturbation. Traditional quantum mechanics[7] gives the second-order energy correction as

$$E_n = E_{0,n} + \langle\psi_{0,n}|H_1|\psi_{0,n}\rangle - \sum_{k\neq n}\frac{\left|\langle\psi_{0,k}|H_1|\psi_{0,n}\rangle\right|^2}{E_{0,n}-E_{0,k}} \, , \tag{4}$$

and the first-order correction of the wave function as

$$\psi_n = \psi_{0,n} + \sum_{k\neq n}\frac{\langle\psi_{0,k}|H_1|\psi_{0,n}\rangle}{E_{0,n}-E_{0,k}}\psi_{0,k} \quad . \tag{5}$$

Later, we will apply the one-dimensional Schrödinger equation with a potential $V(x)$:

$$-\frac{\hbar^2}{2m}\frac{\partial \psi_n}{\partial x^2}+V(x)\psi_n=E_n\psi_n \quad , \tag{6}$$

where $\hbar$ is the Planck constant and m is the mass of the particle that follows Eq. (6). Comparing Eqs. (3) and (6), we find the general relations

$$H_0=-\frac{\hbar^2}{2m}\frac{\partial^2}{\partial x^2} \quad , \quad H_1=V \, , \quad H=H_0+V \, . \tag{7}$$

Therefore, we expand the perturbation with respect to *V*.

3 PERTURBATION THEORY FOR WEBSTER'S EQUATION[8,9]

To clarify the resemblance between the Webster's and Schrödinger equations, we try a change of variables in Webster's equation (1) as follows:

$$\Psi_n(x,t)=P_n(x,t)\sqrt{S(x)} \tag{8}$$

$$r(x)=\sqrt{S(x)} \quad , \tag{9}$$

where *r* is clearly proportional to the radius of its cross-section at *x*. The time dependence of *P* is separated by the factor $e^{i\omega t}$

$$P_n(x,t)=\tilde{P}_n(x)e^{i\omega t} \, . \tag{10}$$

Here ω is the angular frequency and

$$k=\frac{\omega}{c} \tag{11}$$

is the wavenumber of the wave. The equation (1) then transforms into

$$-\frac{d^2\psi_n}{dx^2}+\frac{r''}{r}\psi_n={k_n}^2\psi_n \, , \tag{12}$$

where the eigen- "wavefunction": $\psi_n(x)$ is also introduced as

$$\Psi_n(x,t)=\psi_n(x)e^{i\omega t} \tag{13}$$

Putting $E_n={k_n}^2$ and $\hbar=2m=1$, we obtain Schrödinger equation for one dimensional scattering (6), where ${k_n}^2$ expresses the energy of the particle and the potential energy $V(x)$ becomes r''/r. Note that n labels the eigen-wavenumber k_n and the eigen-energy E_n in a finite region, i.e., within the space of the brass instrument. The Hamiltonian of the system becomes

$$H=H_0+V=-\frac{d^2}{dx^2}+\frac{r''}{r} \quad . \tag{14}$$

Thus, the potential energy term r''/r plays a perturbative role.

Different from Schrödinger equation, we do not normalize $\psi_n(x)$, because the term $\psi_n(x)/\sqrt{S(x)}$ represents the sound pressure at *x*. Therefore, the normalization would remove some important information.

Perturbation theory is applicable when the contribution of the perturbation $H_1=V=r''/r$ is relatively small. To obtain the difference between ${k_{0,n}}^2$ of the straight pipe and ${k_n}^2$ with a second-order perturbation *V*, we modify Eqs. (4) and (5) as

$${k_n}^2={k_0}^2+{\gamma_n}^{-1}\left\langle\psi_{0,n}\left|\frac{r''}{r}\right|\psi_{0,n}\right\rangle-\sum_{m\neq n}{\gamma_k}^{-1}\frac{\left|\left\langle\psi_{0,m}\left|\frac{r''}{r}\right|\psi_{0,n}\right\rangle\right|^2}{{k_{0,n}}^2-{k_{0,m}}^2}{\gamma_n}^{-1} \, , \tag{15}$$

$$\psi_n=\psi_{0,n}+\sum_{m\neq n}\frac{\left\langle\psi_{0,m}\left|\frac{r''}{r}\right|\psi_{0,n}\right\rangle}{{k_{0,n}}^2-{k_{0,m}}^2}{\gamma_n}^{-1}\psi_{0,n} \quad , \tag{16}$$

where the symbols in (15) and (16) are respectively defined as

$$\left\langle\psi_{0,n}\left|\frac{r''}{r}\right|\psi_{0,m}\right\rangle\equiv\int_a^b\psi_{0,n}\frac{r''}{r}\psi_{0,m}dx \tag{17}$$

and

$$\gamma_n\equiv\int_a^b{\psi_{0,n}}^2dx \quad . \tag{18}$$

The factor γ_n is introduced for acoustical applications. In quantum mechanics, the wavefunctions ψ_n must be normalized as $\gamma_n=1$, because $\psi_n(x)^2\,dx$ represents the probability that a corresponding particle exists in the range $[x,x+dx]$. Therefore, integrating all probabilities of a particle existing in that region, we obtain

$$\int_a^b{\psi_n}^2dx=1 \quad , \tag{19}$$

implying that the particle is somewhere inside the whole range $[a,b]$.

As a non-perturbative system, we solve Webster's equation in a straight pipe. The non-perturbative system should be solvable and admit a series of analytical and exact solutions $\psi_n(x)$.

A straight-pipe system is obtained by neglecting the potential energy term r''/r. The solution of the non-perturbed Eq. (12) is

$$\psi_{0,n}(x)=A_n\cos\left(k_{0,n}x\right)+B_n\sin\left(k_{0,n}x\right) \, . \tag{20}$$

The boundary condition quantizes the wavenumber *k*. The general solution for the straight pipe, obtained by summing the k_n, is the following Fourier decomposition, as expected:

$$\psi_0(x) = \sum_n \psi_{0,n}(x) = \sum_n \left\{ A_n \cos\left(k_{0,n}x\right) + B_n \sin\left(k_{0,n}x\right) \right\}. \quad (21)$$

As the horn is open-ended at both sides, ψ must be 0 at both ends $x=a$ and $x=b$. Thus, the boundary conditions are $\tan\left(k_{0,n}a\right) = \tan\left(k_{0,n}b\right) = -A_n/B_n$; equivalently, $\sin\left\{k(b-a)\right\} = 0$. Thus, the wavenumbers are quantized as

$$k_{0,n} = \frac{n\pi}{b-a} = \frac{n\pi}{L}. \quad (22)$$

Under this boundary condition, Eq. (21) becomes

$$\psi_0 = \sum_n B_n \left\{ \sin\left(k_{0,n}x\right) - \tan\left(k_{0,n}\right)\cos\left(k_{0,n}x\right) \right\}. \quad (23)$$

Eq. (22) also offers the eigen-frequency $f_{0,n} = ck_{0,n}/2\pi = cn/2(b-a)$ of the sound wave in the straight pipe.

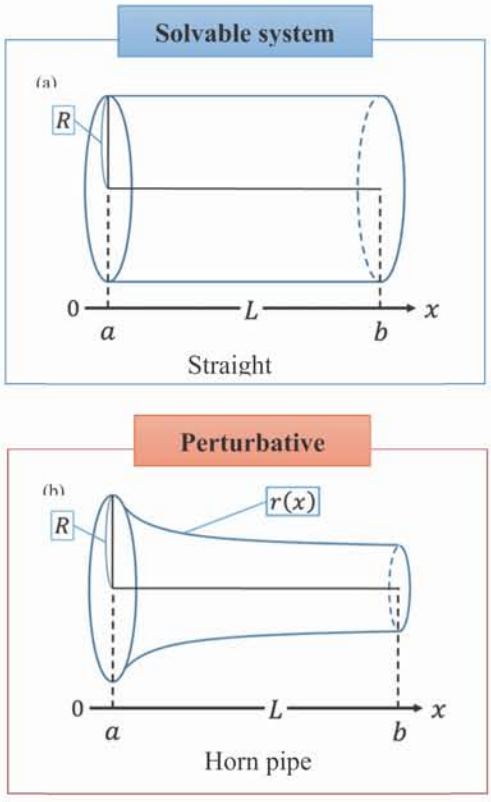

FIG. 2. Schematics of (a) a solvable straight pipe and (b) a perturbative pipe. The x-coordinate is aligned along the rotational symmetry axis of the horn. In both cases, $r(a) = R$ and $b-a = L$.

4 NUMERICAL CALCULATION MODELS

The shape of a horn pipe can be modeled by various functions. In this paper, we apply perturbation theory to horns of various shapes. Each shape is determined by rotating a body defined by the function r(x) around the x-axis. For each shape, we compare the solutions of the straight pipe and the varying horn (calculated by perturbation theory)(FIG.2). The solutions are also compared with those of typical numerical methods. If the exact solution is obtainable, comparisons between the exact and perturbative solutions will validate or invalidate the perturbation method.

To test the accuracy and efficiency of our method, we compare our results with those of FEM10,11. The lattice constant is set to $\Delta x = 0.001$. The energy $E = k^2$ is incremented by $\Delta E = \Delta(k^2) = 0.0002$, and the eigenstates are searched.

The accuracy of FEM usually deteriorates at higher energies, where the wavelength becomes comparable to or smaller than the lattice constant Δx. Therefore, computational approaches can only roughly approximate the physical phenomena in high-energy regions. The lattice constant must be set sufficiently small to prevent this degradation. The wavelength of the non-perturbative system $\lambda_{0,n} = 2\pi/k_{0,n} = 2L/n$ reduces as L shortens and/or n increases. In our work, the shortest wavelength is $\lambda_{0,30} = 2\times 1/30 = 0.06667... \gg \Delta x$ for $L = 1$ and n = 30. Note that $\lambda_{0,30}$ is more than sixty times larger than Δx.

The x-coordinate of Webster's equation must align along the axis of rotational symmetry of the pipe (namely, through the center of the pipe). In the perturbative systems, the shapes of the horn pipe are given by the following functions (see FIG. 3):

(a) $r(x) = e^{-x}$
(b) $r(x) = 1/x$
(c) $r(x) = 3 + \cos x$
(d) $r(x) = \ln x$. (24)

The left and right ends of the pipe are located at $x=a$ and $x=b$, respectively. The pipe length is $L=b-a$. To ensure that the pipe shape changes gradually along its length, we select $L = 1, 2, \ldots, 10$, and determine the wavenumbers k_n and wavefunctions ψ_n for $n = 1, 2, \ldots, 30$.

The end positions are set to $a=0$, $b=L$ for potential shapes (a) and (c), $a=1, b=L+1$ for shape (b) and $a=e, b=e+L$ for shape (d). When $a=0$, the boundary conditions reduce to the simple forms $A_n \equiv 0$ and $\tan\left(k_n{}^0\, b\right) = 0$, and the result becomes Eq. (22).

This section focuses on ψ_n rather than $P_n = \psi_n/\sqrt{S}$, because the effect of varying the radius is much easier to distinguish in ψ_n than in pressure. Different from their usual

definitions, both "energy" and "potential" have units of m^{-2} and are so named only by mathematical analogy between the Webster's and the Schrödinger equations.

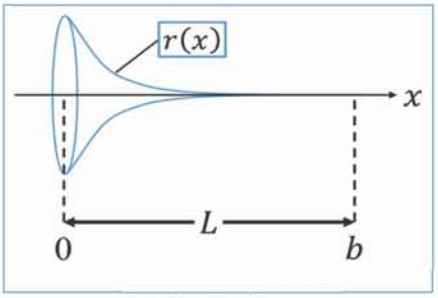

$r(x)=e^{-x}$ (a)

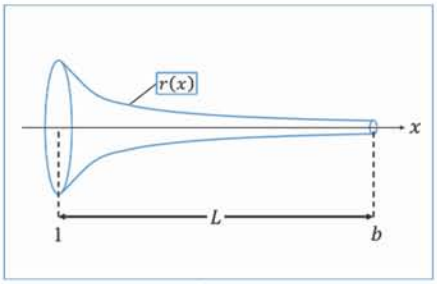

$r(x)=\frac{1}{x}$

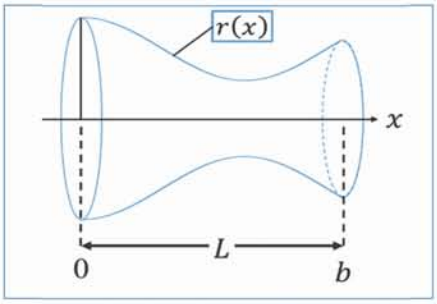

$r(x)=3+\cos x$

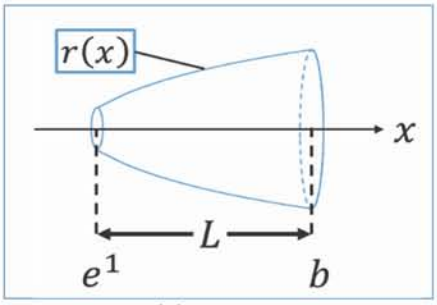

$r(x)=\ln x$

FIG.3. Schematics of the pipe shapes investigated in the perturbation study: (a) $r(x)=e^{-x}$, (b) $r(x)=1/x$, (c) $r(x)=3+\cos x$, (d) $r(x)=\ln x$.

A. Potential (a): $r(x) = e^{-x}$

In this case $r''/r=1$ is a constant "potential", and Webster's equation becomes

$$-\frac{d^2\psi_n}{dx^2}=\left(k_n{}^2-1\right)\psi_n\,. \tag{25}$$

The spectrum is essentially that of the straight-pipe potential $r(x)\equiv 0$ (FIG. 4), but with $k_n{}^2$, in the right-hand side replaced by $k_n{}^2-1$. Similarly, the "eigen-energies" of $r(x)=e^{-x}$ are those of the straight pipe shifted by -1. The "energies" of the perturbation results differ from the exact solution by

$$\Delta E_n{}^2=\left\{\left(k_n^{\mathrm{ext}}\right)^2-\left(k_n^{\mathrm{Pert}}\right)^2\right\}^2\,, \tag{26}$$

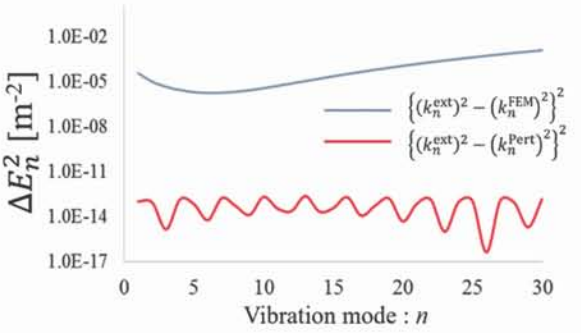

(a) L=1

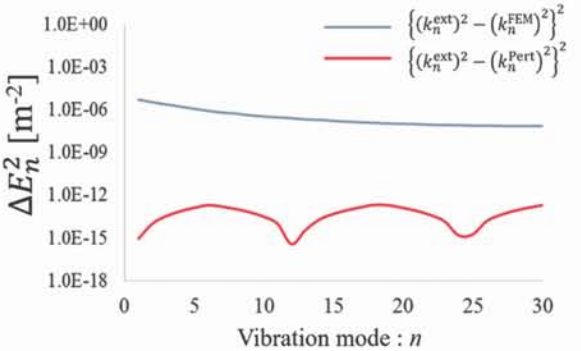

(b) L=8

FIG. 4. With $r(x)=e^{-x}$, squares of eigen energy($k_n{}^2$) deviations by the perturbation method and FEM from the exact solution are illustrated: (a) L=1, (b) L=8. The deviations of FEM are almost 10^{10} times larger than the perturbation. The deviations $\Delta E_n{}^2$ are defined in Eqs. (26) and (27).

where $k_n^{\mathrm{ext}}=\sqrt{k_{0,n}{}^2-1}$ is the exact solution of Eq. (25), and k_n^{Pert} is the wavenumber derived by our method, setting the "potential" $r''/r=1$. The FEM results $k_n{}^{\mathrm{FEM}}$ differ from the exact solution by

$$\Delta {E_n}^2 = \left\{ \left(k_n^{\mathrm{ext}}\right)^2 - \left(k_n^{\mathrm{FEM}}\right)^2 \right\}^2 , \tag{27}$$

where k_n^{FEM} is the wavenumber obtained by FEM.

The calculation which can be estimated in this case, because the exact solution is obtainable. The deviation result $\Delta {E_n}^2$ of the perturbation method is strikingly superior (by 10 orders of magnitude) to the FEM result. The deviations from the exact squared "energies" approach the precision limit of the computational program (FIG. 4). Of course, the wavefunctions are identical to those in a straight pipe.

B. Potential (b): $r(x)=1/x$

In this case, $r''/r = 2/x^2$ is a monotonically decreasing function of x. This case is also exceptional, because its equation

$$-\frac{d^2\psi_n}{dx^2} + \frac{1}{x^2}\psi_n = {k_n}^2\psi_n \ . \tag{28}$$

can be solved analytically. The solutions are linear combinations of the Bessel function $J_{\frac{3}{2}}(x) = \sqrt{\frac{2}{\pi x}}\left(\frac{\sin x}{x} - \cos x\right)$ and the Neumann function

$$N_{\frac{3}{2}}(x) = J_{-\frac{3}{2}}(x) = -\sqrt{\frac{2}{\pi x}}\left(\sin x + \frac{\cos x}{x}\right):$$

$$\psi_n(x) = A_n J_{\frac{3}{2}}(k_n x) + B_n N_{\frac{3}{2}}(k_n x) \ . \tag{29}$$

The boundary condition $\psi_n(a) = \psi_n(b) = 0$ then becomes

$$\frac{N_{\frac{3}{2}}(k_n a)}{J_{\frac{3}{2}}(k_n a)} = \frac{N_{\frac{3}{2}}(k_n b)}{J_{\frac{3}{2}}(k_n b)} = -\frac{A_n}{B_n} \tag{30}$$

and k_n is properly determined[8]. In terms of k_n, the boundary condition is written as

$$\tan\{k_n(b-a)\} = \frac{k_n(a+b)}{{k_n}^2 ab - 1} \ . \tag{31}$$

The exact spectrum can be numerically computed by Eq. (31). The squared eigen-energy deviations (relative to the exact solution) are plotted in FIG. 5. Again, the spectrum computed by the perturbation method is almost perfect. The error approaches the precision limit of the computer program, especially at shorter lengths(FIG. 5 (a)). The wavefunctions are also well evaluated (FIGs. 6 and 7). When L is small, the "potential" exerts negligible effect because the "energy" is high. On the other hand, larger L reduces the "energy" and the wavefunction becomes more sensitive to the "potential". In fact, as ${k_n}^2 \approx {k_{0,n}}^2 = (n\pi/L)^2$, the "energy" is roughly proportional to the inverse square of the length of the pipe: L^{-2}. For fixed L, the distortion becomes more serious as n reduces.

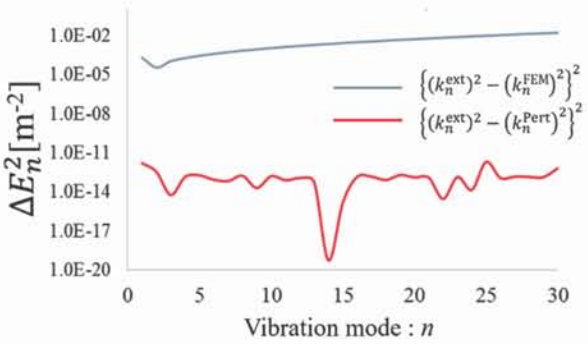

(a) L=1

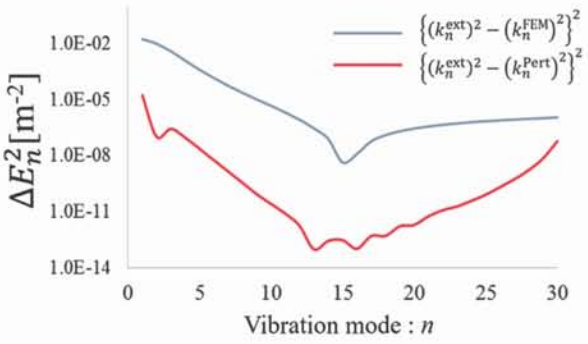

(b) L=10

FIG. 5. Potential $r(x) = 1/x$. Shown are the squared eigenenergies (k_n^2) calculated by the perturbation method and FEM, relative to the exact solution: (a) L=1, (b) L=10.

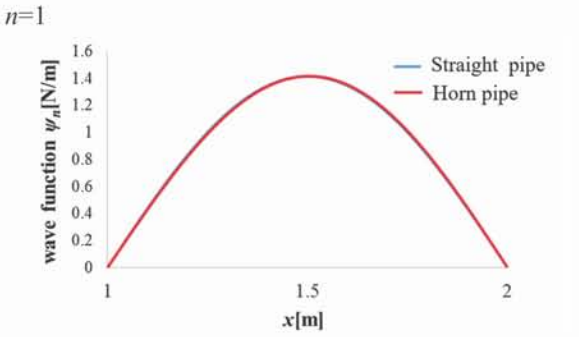

(a) L=1

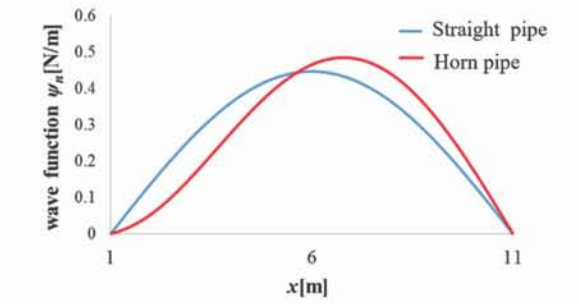

(b) L=10

FIG. 6. Potential $r(x) = 1/x$, showing the wave- functions $\psi_{n=1}$ in the horn pipe and straight pipe for: (a) L=1, (b) L=10.

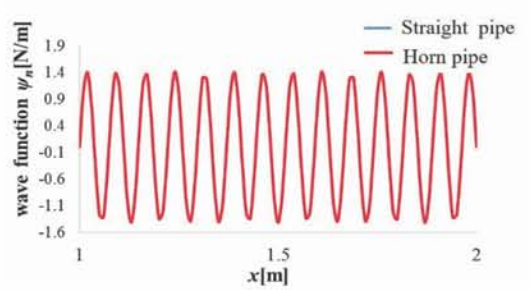

(a) L=1

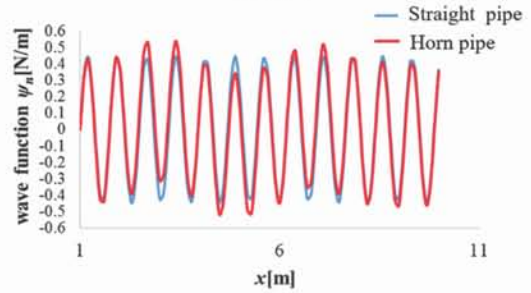

(b) L=10

FIG. 7. Potential $r(x)$ = $1/x$, showing the wave- functions $\psi_{n=27}$ in the horn pipe and straight pipe for: (a) L=1, (b) L=10

. Potential (c): $r(x)=3+\cos x$

In this case, the "potential" r''/r becomes

$$\frac{r''}{r}=-\frac{\cos x}{3+\cos x}=-\frac{1}{1+\dfrac{3}{\cos x}} \quad . \tag{32}$$

This is a periodic function with period 2π (FIG. 8). Different from the three other potentials examined in this work, which are monotonically decreasing or increasing, this potential imposes its periodicity on the wavefunction. In quantum mechanical terms, this potential describes one-dimensional scattering.

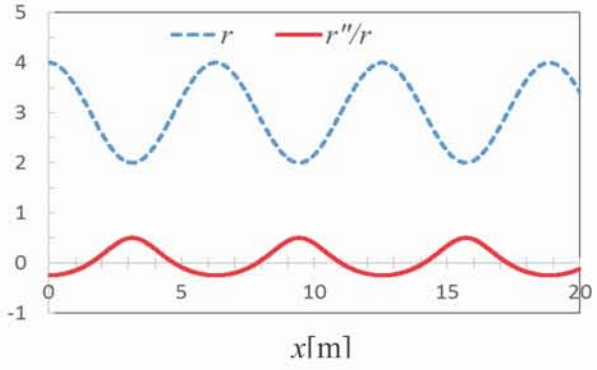

FIG. 8. Pipe radius $r(x)=3+\cos x$ and "potential " $r''/r=-\cos x/(3+\cos x)$ are plotted for pipe shape (c).

In the case n=1 (FIG. 9), the "energy" is approximately calculated as $k_1^2 \approx k_{0,1}^2=(\pi/L)^2$. When L=1, the energy becomes $k_1^2=\pi^2\approx 9.870\ldots$, much larger than the "potential" energies, which range from -0.25 to 0.5. Therefore, the "potential" exerts minimal effect on the wavefunction. However, in the longer pipe with L=10, the "energy" deceases to $k_1^2 \approx (\pi/10)^2 \approx 0.09870\ldots$, in the middle of the

n=1

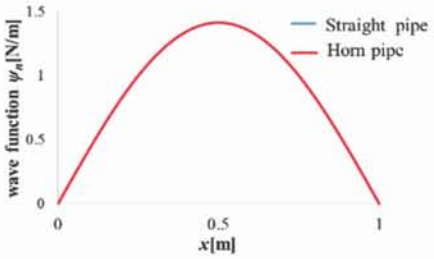

(a) L=1

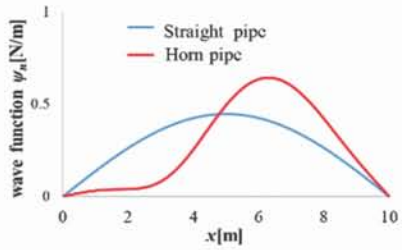

(b) L=10

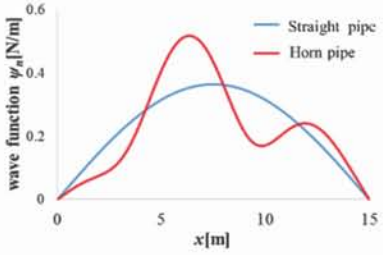

(c) L=15

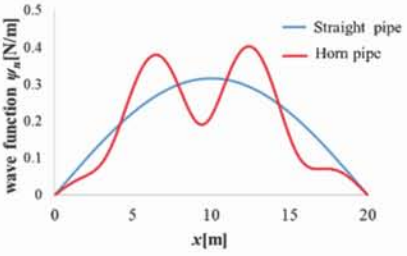

(d) L=20

FIG. 9. Potential $r(x)=3+\cos x$, showing the wave functions $\psi_{n=1}$ for (a) L=1, (b) L=10, (c) L=15 and (d) L=20. The peaks of the wave- functions appear close to the bottoms of the potentials: $x=2\pi(=6.283...)$, $4\pi(=12.57...)$ and $6\pi(=18.85...)$.

"potential" energy range (32). Consequently, the wavefunction is enhanced near the bottom of the "potential" r''/r, and diminished around the peaks. In quantum mechanical terms, the wavefunction defines the probability that a particle will be found at a specific point in the system. The peaks indicate regions of low probability of finding a particle. Particles are most likely to exist in the bottoms of the "potentials".

In FIG. 9, the waves in longer horns exhibit multiple peaks imposed by the periodic "potential". All wavenumbers are $n=1$, denoting ground states or first modes. The pressure $P(x,t)$ can be enumerated from the wavefunction $\psi_n(x,t)$ by Eq. (8). The pressures exhibit a single peak (FIG. 10), which typifies the first mode in a finite region.

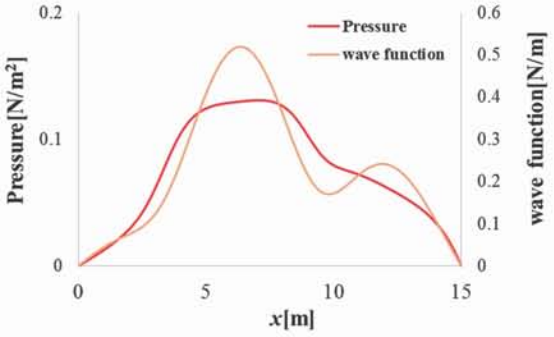

FIG. 10. Pressure $P(x)$ and wavefunction $\psi_n(x)$ in the potential $r''/r=-\cos x/(3+\cos x)$ with n=1 and L=15. The pressure has just a single peak, although it is quite distorted.

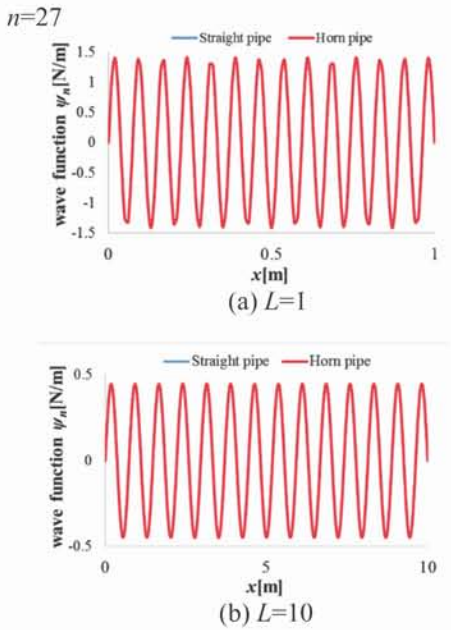

FIG. 11. Potential $r(x)=3+\cos x$, showing the wavefunctions $\psi_{n=27}$ for: (a) L = 1 and (b) L = 10. In case (b), the wavefunction is slightly affected by the "potential".

In the higher mode n=27 (FIG. 11), $k_{27}^2 \approx k_{0,27}^2=(27\pi/L)^2$ exceeds the "potential". For example, if L=1, then $k_{27}^2 \approx k_{0,27}^2=(27\pi)^2 \approx 7200$, outrageously larger than the "potential". In this case, the wavefunction is barely influenced by the "potential" (FIG. 11). Even in the longest horn examined in our work (L=10), $k_{27}^2 \approx 72$ is considerably larger than the "potential". To observe this apparently unusual wave distortion, we require an unrealistically long horn (e.g., L=100).

D. Potential (d): $r(x) = \ln(x)$

The "potential" $r''/r=-1/(x^2 \ln x)$ becomes very small and negative in the range [e, e+L] ($r''/r=-0.1353\ldots$ at $x=e$), and gradually approaches the x-axis. Initially, we simply multiply the representative potential (a) by $-1/\ln x$. Of course, the shape changes drastically toward small x, but this region is discarded. In the valid range, this potential varies much more slowly than the other potentials. As already explained, the energy is also much higher than the potential, so the wavefunction resembles that of the straight pipe over the whole parameter range tested in this study (FIGs. 12 and 13). Nevertheless, the wavefunction slightly distorts in longer systems.

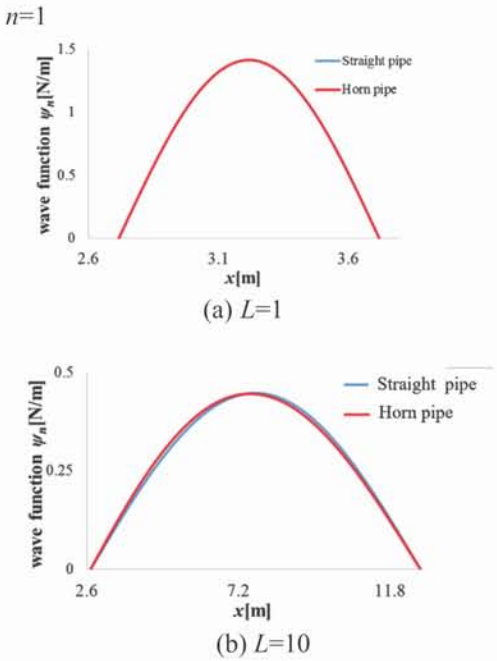

FIG. 12. Potential $r(x)=\ln x$, showing the wavefunctions $\psi_{n=1}$ for (a) L=1 and (b) L=10. The "potential" exerts negligible effect in both length cases.

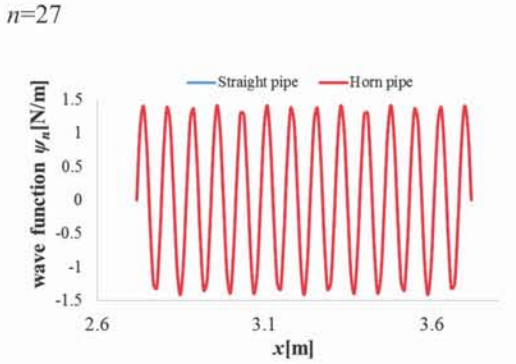

(a) L=1

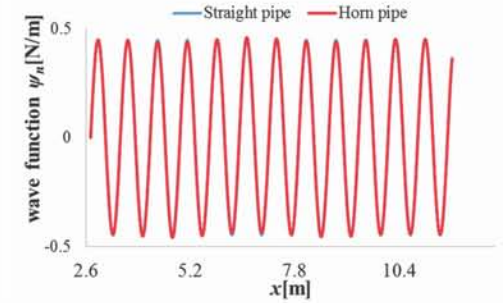

(b) L=10

FIG. 13. With $r(x)=\ln x$, graphs of wave function $\psi_{n=27}$ are illustrated in the cases : (a) L=1, (b) L=10. The effect of the "potential" is really limited.

5 SUNNARY AND DISCUSSIONS

This paper applies perturbation theory to Webster's equation (1), and derives second-order perturbation expression for horns of various shapes. Successful application of the theory to Webster's equation was confirmed in comparisons with the exact solutions. The wave number k_n and the sound pressure $P_n=\psi_n/\sqrt{S}$ were correctly enumerated. Moreover, this method was applicable to pipes that markedly deviated from the straight pipe (the simplest solvable shape). Moreover, this method was viable for variously shaped brass instruments.

The calculation can be performed at much higher precision, and with remarkably less numerical computation, than FEM. On a paralleled workstation of several CPUs constructed in our laboratory, the FEM required 20–30 minutes' runtime for each given set of L and n. On the other hand, our method enumerates the cross integrations (16) almost instantaneously.

The longer the instrument, the larger the effect of the perturbation, because the wavefunction in the horn becomes more distorted. However, the perturbation method is much more resilient to shapes that deviate from straight pipes than initially expected.

We believe that the exponential horn is the preferred design for brass instruments, because of its nearly flat frequency characteristics1. However, real musical instruments have more delicate structures, for reasons that are not fully understood. When played, the instruments must deliver high-quality sound that changes continuously. Therefore, their dynamical properties must be studied. In subsequent investigations, we will investigate the time dependent characteristics of the horn shapes in a theoretical framework.

The time-dependent acoustical wave equation differs from the quantum Schrödinger equation. The former involves a quadratic time differential, whereas the latter has a first-order time differential. This mathematical difference complicates the analysis, and likely requires a new mathematical approach.[4),16)]

References and Links

1. Eric J. Heller. Why You Hear What You Hear: An Experiential Approach to Sound, Music, and Psychoacoustics. Princeton University Press, Princeton, (2012).
2. Kin'ya Takahashi, Kana Goya, and Saya Goya, "Mode Selection Rules for Two-Delay Systems: Dynamical Explanation for the Function of the Register Hole on the Clarinet", J. Phys. Soc. Jpn. 83, 124003 (2014).
3. Arthur H. Benade, Fundamentals of Musical Acoustics, Dover Publications, 391-411 (1990).
4. Mitsuyoshi Tomiya, Yosuke Sasaki and Shoichi Sakamoto, "Numerical Analysis of Dynamical Scar in Sound Propagation", Proceedings of the 12th Western Pacific Acoustics Conference 2015, P9000179, http://wespac2015singapore.com/eproceedings/html/P9000179.xml (2015).
5. David T. Blackstock, Fundamentals of Physical Acoustics, A Wiley-Interscience publication, 251-254 (2000).
6. P. A. Martin, "On Webster's Horn Equation and Some Generalizations", J. Acoust. Soc. Am. 116, 1381-1388, (2004).
7. Walter Greiner, Quantum Mechanics: An Introduction 4th Edition, Springer-Verlag, Berlin, Heidelberg, New York, 273-277(2001).
8. R. Jorge, arXiv: 1311.4238v1, physics.flu-dyn., (2013).

9. A.H.Benade and E. V. Jansson, “On Plane and Spherical Waves in Horns with Nonuniform I. Flare, “Theory of Radiation, Resonance Frequencies, and Mode Conversion”, Acustica 31(2), 79–98, (1974).
10. Ichiro Kawakami, Masamitsu Aizawa, Katsumi Harada and Hiroyuki Saito, “Finite Element Method for Nonlinear Wave Propagation”, J. Phys. Soc. Jpn. 54, 544-554 (1985).
11. Antoine Lefebvre and Gary P. Scavone, “Characterization of Woodwind Instrument Toneholes with The Finite Element Method”, J. Acoust. Soc. Am. 131(4), 3153-3163 (2012).
12. Roger Waxler, “A Vertical Eigenfunction Expansion for The Propagation of Sound in A Downward-refracting Atmosphere”, J. Acoust. Soc. Am. 112(8), 2541-2552 (2002).
13. Yusuke Naka, Assad A. Oberai and Barbara G. Shinn-Cunningham, “Acoustic Eigenvalues of Rectangular Rooms with Arbitrary Wall Impedances Using The Interval Newton/generalized Bisection Method”, J. Acoust. Soc. Am. 118(6), 3662-3671 (2005).
14. Roger R. Bate, Fundamentals of Astrophysics, Dover Publications, 385-427 (1971).
15. A. G. Webster, “Acoustical Impedance, and The Theory of Horns and of The Phonograph,” Proc. Natl. Acad. Sci. U.S.A. 5, 275–282 (1919).
16. Keita Hamano, Shoichi Sakamoto and Mitsuyoshi Tomiya, “High Accuracy Solution and Shape Universality of Webster’s Equation in High Frequency Region by Perturbation Theory”, Proceedings of the 12th Western Pacific Acoustics Conference 2015, P9000185, http://wespac2015singapore.com/eproceedings/html/ P9000185.xml (2015).